A NEW METHOD FOR ACCURATE MEASUREMENTS OF THE LUMPED SERIES RESISTANCE OF SOLAR CELLS

A.G. Aberle, S.R Wenham and M.A. Green
Centre for Photovoltaic Devices and Systems
University of New South Wales, Kensington NSW 2033, Australia

ABSTRACT

Measurements of the series resistance R_s are important for the localisation of dominant loss mechanisms in photovoltaic devices. The new measurement technique presented in this work uses the measured "J_{sc}-V_{oc} *curve*" of a solar cell as an approximation to the unknown R_s-corrected *I-V* curve and determines the "*lumped series resistance*" in dark and illuminated operating conditions ($R_{s.dark}$ and $R_{s.light}$) from the voltage shift between the "J_{sc}-V_{oc} *curve*" and the dark and illuminated *I-V* curve, respectively. Owing to multi-dimensional effects in practical devices, the lumped series resistance depends on the operating condition of the cell (i.e., dark or illuminated *I-V* measurements) and on the current density flowing through the device.

This work not only provides a new, powerful method for the determination of the lumped series resistance of photovoltaic devices, but also considerably improves the general understanding of ohmic power loss effects in silicon solar cells.

1. INTRODUCTION

Photovoltaic devices are low-voltage, high-current power generators. For instance, under one-sun illumination, a commercially available 19% efficient 45 cm^2 silicon solar cell produces about 1.6 A of current at an operating voltage slightly above 0.5 V. Owing to the large output currents, the minimisation of ohmic series resistance losses is of vital importance for high energy conversion efficiencies of solar cells. In a *conventional* solar cell (i.e., a cell with a current-collecting emitter along the illuminated front surface and a comb-like front electrode), ohmic losses arise from the limited conductivity of the metal contacts, the metal-semiconductor contact resistance, the substrate resistance, and the emitter sheet resistance.

A severe complication in the determination of series resistance losses of solar cells arises from the fact that the losses associated with the emitter sheet resistance and the substrate resistance are distributed by nature and current flow patterns are usually different in dark and illuminated *I-V* measurements. Fig. 1 illustrates the effect for a n^+p silicon solar cell. Owing to the completely metallised rear surface of this cell, the 2-dimensional (2D) current flow in Fig. 1 is fully attributed to the emitter sheet resistivity. In dark *I-V* measurements, a voltage V is externally applied to the cell electrodes. However, due to the emitter sheet resistance, the operating voltage along the emitter surface is not constant but *decreases* towards the central emitter region (i.e., is smallest in the middle between two front metal fingers). Consequently, the injected forward-current density is larger in the cell regions close to the top metal fingers, compared to the central device region. Under illumination, the current flow in the cell is reversed, leading to an *increased* operating voltage in the central emitter region. As can be seen from Fig. 1, for similar external currents, the current density in the central emitter region is smaller in dark *I-V* measurements than under illumination, and consequently the "dark" resistive losses of the device are smaller than those under illumination.

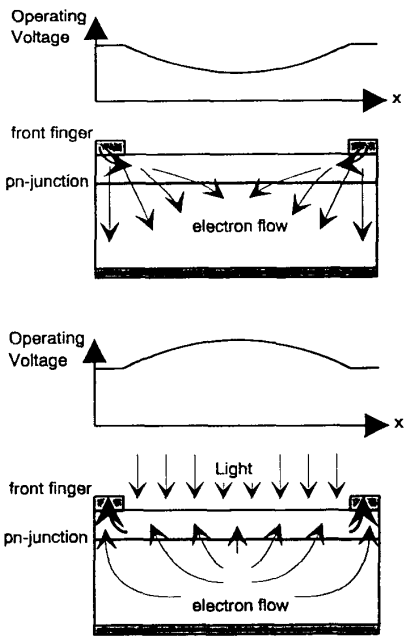

Fig. 1 Schematic representation of the 2-dimensional electron flow pattern in a n^+p Si solar cell in dark *I-V* measurements (top) and under uniform illumination (below).

In order to quantitatively assess the resistive losses of a solar cell, the simple equivalent circuit of Fig. 2 is usually applied. All resistive losses in the cell are lumped into a single "*lumped series resistance*" R_s which is in series with the load and produces an ohmic power loss of I^2R_s when a current I flows through the device. As R_s depends on the operating condition of the cell (see Fig. 1), the lumped series resistance in dark *I-V* measurements will subsequently be referred to as $R_{s.dark}$, while the corresponding illuminated parameter is $R_{s.light}$.

0-7803-1220-1/93 $3.00

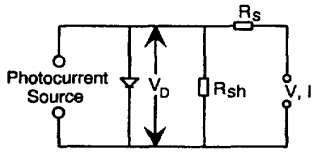

Fig. 2 Basic equivalent circuit of a solar cell. All resistive losses in the device are lumped into a single resistance R_s.

The series resistance problem of solar cells has intensively been investigated in the past [1-7], very often, however, under the erroneous assumptions of a spatially constant diode voltage along the top surface and a uniform current generation. Probably the most comprehensive theoretical study including the impact of the emitter voltage drop of Fig. 1 on cell series resistance in dark and illuminated *I-V* measurements has been performed by Nielsen [6]. In order to calculate the spatial variation of diode voltage and sheet current density, the 1D-study assumes a perfectly conducting substrate and neglects the influence of base parameters (e.g., geometry, resistivity, carrier lifetime) on the minority carrier flow pattern in the device. Nielsen's work predicts that (i) $R_{s.light} \approx R_{s.dark} \approx constant$ for small currents and (ii) that $R_{s.dark}$ decreases with increasing current. In a subsequent work, Cuevas et al. [7] have shown that a similar behaviour results from the "*metal-covered diode effect*". By assuming 2 diodes in parallel (a completely metallised diode and fully illuminated one) which are separated by a resistance, a simple model again predicts a decrease of $R_{s.dark}$ with increasing current and a constant $R_{s.light}$. However, to a degree which depends on the finger spacing and the emitter sheet resistance, $R_{s.light}$ is shown to be larger than $R_{s.dark}$.

The metal-covered diode effect is even more pronounced if the increased surface recombination velocity at the metal-silicon interface is taken into account, as can easily be concluded from assuming two diodes with different saturation currents in parallel. Furthermore, as we have pointed out in a recent study of resistive emitter losses in high-efficiency silicon solar cells [8], resistive power loss effects are more complicated than assumed by the 1D-model of Nielsen [6]. To an extent depending on front finger spacing, emitter sheet resistivity, light concentration, substrate minority carrier lifetime and rear surface passivation quality, the minority carrier flow in the base of the silicon solar cell of Fig. 1 deviates from the simple current flow pattern assumed by 1-dimensional solar cell theory. The 2-dimensional minority carrier flow in the base reduces the lateral emitter current — and thus the resistive emitter losses — below the predictions of 1D-theory. The effect is particularly important for concentrator cells and leads to a reduction of $R_{s.light}$ with increasing current output. Principally, as a result of the large emitter sheet resistance, the current avoids to flow through the emitter layer.

Ohmic voltage drops in the third dimension along the front metal fingers resulting from the limited metal conductivity further increase the difference between $R_{s.dark}$ and $R_{s.light}$ due to the "current-crowding" effect near the contact pad in dark *I-V* measurements (similar to the dark *I-V* case of Fig. 1). Table 1 qualitatively describes the dependence of the lumped series resistance on the operating condition and the current density flowing through the cell for the 3 basic mechanisms mentioned above. In a real device, these mechanisms can be simultaneously present and it is generally very difficult to isolate the influence of each one.

Table 1 Qualitative dependence of R_s on the operating condition and the current density flowing through the solar cell.

Mechanism	*Effect on lumped series resistance*
Emitter sheet resistance effect	- Small currents: $R_{s.dark} = R_{s.light}$ = constant - $R_{s.dark}$ decreases with increasing current - High-efficiency concentrator cells: $R_{s.light}$ decreases with increasing current
Metal-covered diode effect	- $R_{s.light} \approx$ constant - $R_{s.dark}$ decreases with increasing current - $R_{s.light} > R_{s.dark}$ even at small currents
Limited conductivity of front fingers	similarly to metal-covered diode effect

Several measurement techniques have been proposed for the determination of R_s of a solar cell according to the equivalent circuit of Fig. 2. Most commonly, the lumped series resistance $R_{s.dark}$ is obtained from the bending of the semilogarithmic dark *I-V* curve at large currents by means of curve fitting, or from a combination of illuminated and dark *I-V* parameters as proposed by Rohatgi et al. [9] (this approach will be discussed in more detail in Section 2.2). The standard method for the determination of $R_{s.light}$ was developed by Handy [3]. In this approach, the illuminated *I-V* curve of a solar cell is measured at various light intensities and the *I-V* point that lies at a fixed distance from the short-circuit current (e.g., $J = J_{SC}$ - 10 mA/cm^2) is marked on each curve. Ideally, if the diode follows a simple exponential law and the saturation current does not depend on cell voltage, the connection of these points results in a straight line and the series resistance $R_{s.light}$ can be determined from the slope of this line.

Section 2 presents a new, powerful measurement technique for the determination of $R_{s.dark}$ and $R_{s.light}$ as a function of current density. The basic idea of the method is to approximate the unknown R_s-corrected *I-V* curve of the cell by the measured J_{SC}-V_{OC} curve. In order to demonstrate the effectiveness and simplicity of the method, the lumped series resistance of several 1-sun silicon solar cells is determined in Section 3 for dark and illuminated operating conditions.

2. MEASUREMENT PRINCIPLE

Our measurement technique is based on the equivalent circuit of Fig. 2. This simple model of a photovoltaic device consists of a photocurrent source, a diode, a shunt resistance R_{sh} in parallel to the diode and the lumped resistance R_s in series to the diode. In practical solar cells, the impact of the shunt resistance on the *I-V* curve can very often be neglected at normal operating voltages, and the resulting *I-V* characteristics according to this 1-diode model becomes

$$J(V) = J_0\left[exp\left(\frac{V - J\,R_s}{nV_t}\right) - 1\right] - J_L \qquad (1)$$

J_0 is the saturation current density of the diode, n the ideality factor, $V_t=kT/q$ the thermal voltage and J_L the light-generated photocurrent. The sign convention in Eqn. 1 ensures that the dark I-V curve (J_L=0) lies in the first quadrant, while the illuminated I-V curve is in the fourth quadrant. (It has to be mentioned that our method is not limited to the case of a single diode in the equivalent circuit of Fig. 2. In fact, no assumptions on the properties of the diode of Fig. 2 (e.g., single or multi-diode model, exponential I-V characteristics) enter the analysis. Only in order to simplify the following discussion we assume the 1-diode model of Fig. 2).

The measurement technique uses the recognition that the lumped series resistance R_s affects the illuminated and the dark I-V characteristics in differing ways. According to the equivalent circuit of Fig. 2, in the dark I-V case, the voltage at the diode (V_D) is *smaller* than the voltage V at the cell electrodes ($V_D=V-|J|\cdot R_s$), while it is *larger* ($V_D=V+|J|\cdot R_s$) in the illuminated case. Thus, R_s can directly be determined from the voltage shift between the illuminated and dark I-V curve at a given current density. In Section 2.1, the basic features of the new measurement technique are presented for an idealised 1-dimensional solar cell. Section 2.2 includes the modifications of the lumped series resistance imposed by 2-dimensional current flow in practical cells. The saturation current J_0 and the diode ideality factor n of experimental devices can depend on the voltage across the cell. Section 2.3 outlines the complications in the determination of R_s arising from a voltage-dependent saturation current and ideality factor.

2.1 Ideal one-dimensional Case

In the ideal 1-dimensional case, the mechanisms of Table 1 do not exist and the current flow pattern (apart from the current direction) in the cell is identical in dark and illuminated I-V measurements. Thus, the series resistance of the diode is the same for illuminated and dark operating conditions and the voltage shift between the two I-V curves does not depend on the current density. In this case, R_s is simply given by

$$R_s = \frac{\Delta V}{J_{sc}} = \text{constant}, \qquad (2)$$

where J_{sc} is the measured short-circuit current density under illumination. For a graphical determination of the voltage shift ΔV between the two I-V curves it is very convenient to shift the illuminated I-V curve by the photocurrent J_L from the fourth into the first quadrant (Fig. 3). For practical solar cells, J_L can adequately be approximated by the measured short-circuit current density of the device.

2.2 Modifications due to 2-dimensional Current Flow

2.2.1 Imbalance between $R_{s.dark}$ and $R_{s.light}$

As illustrated in Fig. 1, the emitter sheet resistivity produces different current flow patterns in the cell in dark and illuminated I-V measurements. Thus, $R_{s.dark}$ and $R_{s.light}$ can be different and have to be determined separately. At open-circuit conditions, the output current in illuminated I-V measurements is zero and the voltage shift in Fig. 3 between the illuminated and dark I-V curve at the current density $J=J_{sc}$ is completely due to the dark I-V curve. Consequently, $R_{s.dark}$ is given by

$$R_{s.dark}(J = J_{sc}) = \frac{V_{d.jsc} - V_{oc}}{J_{sc}} \qquad (3)$$

where $V_{d.jsc}$ is the "dark" voltage that has to be applied in dark I-V measurements in order to inject the current density J_{sc} into the cell [9]. Conversely, at small currents, the impact of the series resistance on the dark I-V curve is negligible and the voltage shift between illuminated and dark I-V curve is completely due to the illuminated curve. The most important point of the illuminated I-V curve of a solar cell is the *maximum power point* (MPP). The series resistance $R_{s.light}$ determined from the voltage shift between illuminated and dark I-V curve at the maximum power point MPP = (V_{mpp}, J_{mpp}) is given by

$$R_{s.light}(J = J_{mpp}) = \frac{V_{d.mpp} - V_{mpp}}{J_{mpp}} \qquad (4)$$

$V_{d.mpp}$ is the "dark" voltage that has to be applied in dark I-V measurements in order to inject the current density J_{sc}- J_{mpp}.

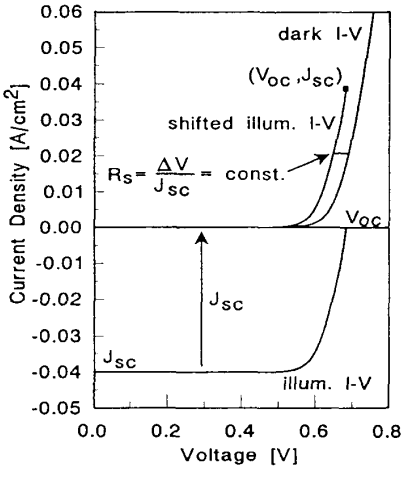

Fig. 3 Measurement principle for the determination of the lumped series resistance R_s of a solar cell from the voltage shift between the dark and illuminated I-V curve. In the assumed case of purely 1-dimensional current flow, the voltage shift between the two I-V curves (and thus R_s) is constant, i.e. does not depend on the current density.

2.2.2 Impact of Current Density

As mentioned in Section 1, the distributed nature of the emitter sheet resistance and the metal-covered diode effect furthermore result in a dependence of R_s on the current density flowing through the device. For a comprehensive determination of $R_{s.light}$ and $R_{s.dark}$ as a function of current density, the R_s-corrected I-V curve of the device should be known. At small currents, the dark I-V curve represents a good approximation to

the R_s-corrected curve, whereas the point (V_{oc}, J_{sc}) in Fig. 3 represents a single point at larger currents which is not affected by R_s. In order to cover the whole current range, we propose to measure the "*J_{sc}-V_{oc} curve*" of the cell (Fig. 4). Experimentally, this curve is obtained by measuring the short-circuit current density J_{sc} and the open-circuit voltage V_{oc} at various light intensities. As neither J_{sc} nor V_{oc} of practical solar cells are affected by series resistance losses, the plot of J_{sc} as a function of V_{oc} is a first-order approximation to the real R_s-corrected I-V curve of the device. With this interpretation, the dependence of $R_{s.dark}$ on current density can be calculated from the voltage shift between the dark *I-V* curve and the J_{sc}-V_{oc} curve at any current level in Fig. 4:

$$R_{s.dark}(J) = \frac{\Delta V(J)}{J} \qquad (5)$$

In the illuminated case one has to keep in mind that the illuminated *I-V* curve was originally measured in the fourth quadrant. Consequently, the actually flowing "lighted" current at a given current density J in Fig. 4 is J_{sc}-J and the dependence of $R_{s.light}$ on current density is given by

$$R_{s.light}(J) = \frac{\Delta V(J)}{J_{sc} - J} \qquad (6)$$

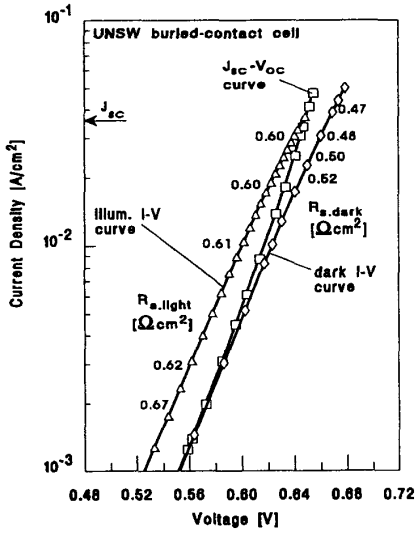

Fig. 4 Exp. determination of $R_{s.light}$ and $R_{s.dark}$ of a 45 cm^2 1-sun BC Si solar cell as a function of current density using the "*J_{sc}-V_{oc} curve*" as an approximation to the unknown R_s-corrected *I-V* curve .

In Fig. 4, the experimental determination of $R_{s.light}$ and $R_{s.dark}$ as a function of current according to Eqns. 5 and 6 is demonstrated for a 45 cm^2 "*buried-contact*" (BC) Si solar cell [10,11] made at the University of New South Wales (UNSW). The measured large difference between $R_{s.light}$ (at the maximum power point) and $R_{s.dark}$ of this cell (41%) reveals the importance of an independent determination of both R_s parameters.

2.3 Complications due to voltage-dependent Saturation Current

As outlined above, our method uses the J_{sc}-V_{oc} curve in order to approximate the unknown R_s-corrected *I-V* curve of the cell. If the saturation current J_0 and the ideality factor n in Eqn. 1 are constant (i.e., do not depend on the voltage across the cell), the J_{sc}-V_{oc} curve *is* the R_s-corrected *I-V* curve of the cell and the accuracy of our R_s-method is solely limited by measurement errors in the determination of the involved *I-V* curves. In real devices, however, J_0 and n very often depend on the voltage across the cell. A critical parameter determining the voltage-dependence of J_0 is the excess minority carrier density in the base (Δn in the case of p-type substrate). With increasing Δn, J_0 of solar cells usually decreases due to the onset of high-injection conditions in the base (e.g. see [12,13]). This behaviour can influence the accuracy of our R_s-method. To be specific, we will discuss the problem for a one-sun n$^+$p high-efficiency silicon solar cell under the idealised assumption of a uniform minority carrier concentration Δn throughout the base.

In dark *I-V* measurements, Δn is fully determined by the voltage across the cell. To a high degree of accuracy this is also true for the J_{sc}-V_{oc} curve, because all voltages of this curve are measured at V_{oc} conditions and the short-circuit current (which is measured at smaller Δn values) of silicon solar cells is only weakly dependent on the recombination parameters in the base (i.e., lifetime and rear surface recombination velocity; these can change with decreasing Δn). Consequently, as similar voltages in the dark *I-V* curve and the J_{sc}-V_{oc} curve correspond to similar Δn values, an injection-level dependent J_0 will equally affect both *I-V* curves, and the proposed method for the determination of $R_{s.dark}$ is only very weakly influenced by an injection-level dependence of J_0.

In illuminated *I-V* measurements, however, the situation is different because Δn is mainly determined by the light intensity, and only to a smaller extent by the voltage across the cell. For instance, if the operating condition in the one-sun *I-V* curve of Fig. 4 is varied from open-circuit to maximum power point (which corresponds to a voltage reduction of about 100 mV), silicon solar cell theory shows that Δn reduces only by a factor of 3 - 5. Conversely, the corresponding point of the J_{sc}-V_{oc} curve ($J \approx 1$ mA/cm^2 in Fig. 4) is obtained for a light intensity of only about 1/40 sun, as can be concluded from assuming a linear dependence between J_{sc} and light intensity. This indicates that Δn at one-sun maximum power point conditions is much larger than at comparable operating voltages in J_{sc}-V_{oc} or dark *I-V* measurements. If the saturation current decreases strongly with increasing Δn, the J_{sc}-V_{oc} curve represents a too pessimistic approximation of the real R_s-corrected *I-V* curve (i.e., the real R_s-corrected *I-V* curve lies to the right-hand side of the J_{sc}-V_{oc} curve in Fig. 4) and our measurement technique will underestimate $R_{s.light}$. Obviously, the effect is most important near maximum power point conditions and diminishes towards open-circuit conditions. (The modifications of the *I-V* curve due to a voltage-dependent ideality factor can equivalently be described in terms of a voltage-dependent J_0. The voltage-dependence of the ideality factor, however, strongly depends on the particular solar cell under consideration and will not be further discussed here.)

The semilogarithmic dark *I-V* curve can be used to check the voltage-dependence of J_0, because any non-ideal behaviour leads to a deviation from the ideal straight-line *I-V* curve. If, in the critical voltage range (600 - 700 mV in the case of one-sun high-efficiency Si solar cells), the semilogarithmic dark *I-V* curve strongly deviates from the straight-line behaviour, the determination of $R_{s.light}$ should be performed closer to the open-circuit voltage. To clarify the situation, a silicon solar cell showing an unusually strong improvement of J_0 with increasing Δn (see [14]) will be investigated in Section 3.2.

3. RESULTS

3.1 Numerical two-dimensional Solar Cell Simulations

In order to quantitatively investigate the impact of the mechanisms of Table 1 on the lumped series resistance, we have performed 2D-simulations of a high-efficiency n^+pp^+ back-surface-field Si solar cell using the numerical device simulator *Simul* [15]. The basic features of this program and the difficulties encountered in 2D-simulations of Si solar cells have been outlined in a previous paper [8]. In order to reveal the various effects on R_s resulting from the emitter sheet resistance, we have chosen a cell structure with relatively large ohmic emitter losses (emitter sheet resistivity 440 Ω/□, finger spacing 1.0 mm). The cell has local heavy n^{++} diffusions below the front fingers for minimised metal contact recombination. Table 2 summarises the most important cell parameters.

Table 2 Parameters of the Si solar cell used for the 2D-simulations.

Cell structure	250 µm thick n^+pp^+ Si solar cell, planar front and rear surface, fully metallised rear surface
Substrate	p-Si, 1.0×10^{16} cm^{-3}, 1.4 Ωcm, τ_{SRH} = 0.5 ms
n^+ diffusion	1×10^{18} cm^{-3}, depth=1 µm,440 Ω/□
local n^{++} diffusion	1×10^{19} cm^{-3}, 2 µm deep, 6 µm wide, 11 Ω/□
p^+ BSF diffusion	1×10^{19} cm^{-3}, depth = 5 µm, 45 Ω/□
Front fingers	Spacing 1 mm, width 3 µm, no contact resist.
Electrical AM1.5 parameters	J_{sc} = 40.79 mA/cm^2, V_{oc} = 689.3 mV FF = 81.73%, Eff. = 22.98%

The dark *I-V* curve, the J_{sc}-V_{oc} curve and various illuminated *I-V* curves of the cell of Table 2 have been calculated with *Simul*. Subsequently, the measurement technique of Section 2 was applied to these *I-V* curves in order to determine $R_{s.dark}$ and $R_{s.light}$ as a function of the current density flowing through the cell. Fig. 5 summarises the results. Interestingly, depending on the operating condition, the lumped series resistance of the test solar cell is found to range from 0.07 to 0.39 Ωcm^2. As predicted by Table 1, $R_{s.dark}$ decreases with increasing current. The $R_{s.dark}$ decrease results from increased current flow near the metal fingers (see Fig. 1). This effectively shortens the current flow path in the cell and reduces $R_{s.dark}$. Owing to the exponential diode characteristics, this effect becomes more pronounced at higher operating voltages. The behaviour of $R_{s.light}$ is more complex. According to Fig. 5, for a given light intensity, $R_{s.light}$ depends strongly on the output current (or, equivalently, on the operating voltage). Furthermore, $R_{s.light}$ decreases with increasing light intensity. The maximum $R_{s.light}$ values are found near short-circuit conditions. The reason for this behaviour is again the reduction of the relative current fraction flowing through the emitter of the cell (see Fig. 1). Due to the exponential diode characteristics, the effect is more pronounced at higher operating voltages (i.e. larger light intensities and/or larger cell voltages at a given light intensity). The most important R_s value, $R_{s.light}$ near the maximum power point, starts to decrease above 0.25 suns.

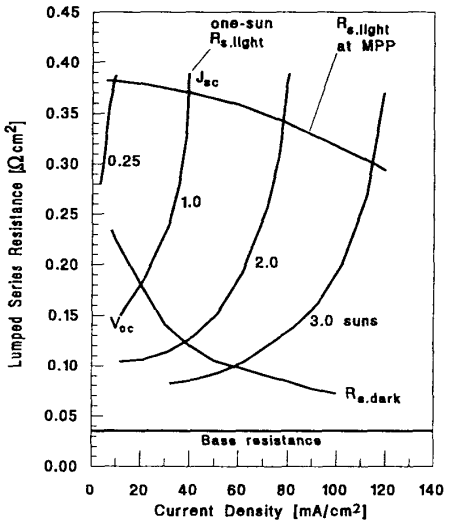

Fig. 5 Dependence of $R_{s.dark}$ and $R_{s.light}$ on the current density flowing through the device obtained from 2D-modelling of the Si solar cell of Table 2. $R_{s.light}$ is shown for 4 different light intensities.

3.2 Experimental Results

In order to demonstrate the effectiveness of the method for a wide range of series resistance values, we have applied the R_S-method of Section 2 to 3 different one-sun high-efficiency Si solar cell structures developed at UNSW. All cells are made on medium-resistivity p-type substrate (≈ 1 Ωcm). The earlier-generation PESC ("*passivated emitter solar cell*") structure [16] has a fully metallised rear surface with an alloyed Al-BSF and a relatively heavy n^+ emitter diffusion. Consequently, series resistance losses in PESC cells generally are small, allowing for very high fill factors. In PERL ("*passivated emitter, rear locally-diffused*") cells [17], which exhibit record efficiencies under AM1.5 illumination, recombination losses are minimised by (i) very small metallisation fractions (mainly due to point contacts at the rear), (ii) heavy diffusions below all metal contacts, and (iii) a light n^+ emitter diffusion. Due to the point-contact metallisation scheme at the rear and the light emitter diffusion, distributed resistance losses are a more severe loss mechanism in PERL cells. In large-area BC ("*buried-contact*") cells [10,11], shading losses as well as resistive losses associated with the front metal grid are minimised by deep, fully metallised grooves. Due to the large finger

spacing (1.2 mm) and the light n^+ emitter diffusion, emitter sheet resistance effects (see Table 1) are expected to be important in BC cells. The measured AM1.5 parameters of the 3 one-sun Si solar cells under investigation and the determined values for $R_{s.dark}$ and $R_{s.light}$ are summarised in Table 3.

Table 3 AM1.5 parameters of the 3 UNSW Si cells under investigation.

Parameter	*PESC*	*PERL*	*BC*
Emitter sheet resist. [Ω/□]	< 150	200 - 400	≈ 200
Finger spacing [mm]	0.8	0.8	1.2
Area [cm^2]	4.0	4.0	45.7
V_{oc} [mV]	661	698	649
J_{sc} [mA/cm^2]	36.6	39.9	37.4
FF [%]	83.0	78.9	79.9
Eff. [%]	20.1	22.0	19.4
$R_{s.dark}$ ($J=J_{sc}$) [Ωcm^2]	0.19	0.38	0.47
$R_{s.light}$ (MPP) [Ωcm^2]	0.20	0.54	0.67

Fig. 6 shows the measured dependence of $R_{s.light}$ and $R_{s.dark}$ on the current density flowing through the device. As expected, owing to the relatively low emitter resistance, the series resistance of the PESC cell does not significantly depend on the operating condition nor the current density: $R_{s.light} \approx R_{s.dark} \approx$ *constant*. The small R_s value (0.20 Ωcm^2) allows for a 1-sun fill factor of 83.0 %, one of the highest values ever measured on UNSW silicon solar cells. Conversely, as a result of the wider finger spacing, the lighter emitter diffusion and the larger cell area, the series resistance of the BC cell under illumination is found to be significantly greater than in the dark (e.g., at 1-sun maximum power point, $R_{s.light}$ is 41% larger than the corresponding $R_{s.dark}$ value). This imbalance indicates (see Table 1) that the metal-covered diode effect and/or the limited conductivity of the metal fingers are very important in BC cells. Technologically, this is due to the ≈ 50 μm deep grooves which lead to effective front grid metallisation fractions of more than 10% and the length of the metal fingers (≈ 60 mm). Furthermore, $R_{s.light}$ as well as $R_{s.dark}$ depend on the current density. The dependence of $R_{s.light}$ on the output current at a given light intensity, which agrees well with the 2D-simulations of Section 3.1, results from the emitter sheet resistance. All 3 effects of Table 1 are believed to cause the decrease of $R_{s.dark}$ with increasing current.

The PERL cell behaves similarly to the buried-contact cell. However, near the maximum power point, $R_{s.light}$ shows a maximum and decreases subsequently with increasing current. This behaviour is attributed to a saturation current J_0 which strongly increases with decreasing voltage across the cell due to an increasing surface recombination velocity at the rear Si-SiO_2 interface [14]. As a result of this voltage-dependent J_0, the J_{sc}-V_{oc} curve is a poor approximation to the ideal R_s-corrected I-V curve near the maximum power point and the R_s-method underestimates $R_{s.light}$ (see Section 2.3). In PERL cells, the imbalance between $R_{s.dark}$ and $R_{s.light}$ is again very large (42%), in spite of the small metallisation fraction of the front metal grid (< 1%). Here, the strong imbalance is due to the large emitter sheet resistivity (which intensifies the metal-covered diode effect (see [7])), additional 2D-effects in the base resulting from the rear point contacts and ohmic voltage drops along the fine metal fingers. According to the $R_{s.light}$ values of Fig. 6, series resistance losses are an important power loss factor in the PERL cell as well as the BC cell, as they reduce the AM1.5 efficiency of these devices by about 0.8 % absolute. The large difference between $R_{s.dark}$ and $R_{s.light}$ in these cells furthermore shows that distributed resistive losses contribute significantly to the total ohmic power losses.

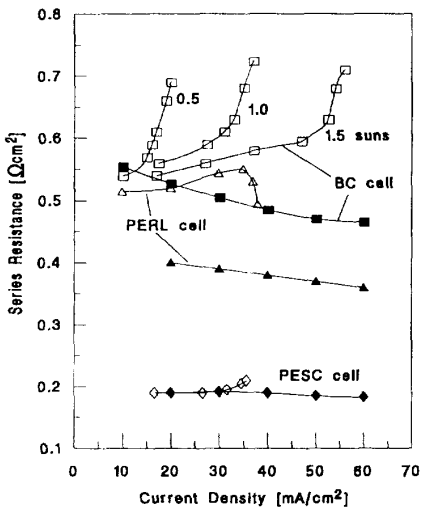

Fig. 6 Measured dependence of $R_{s.light}$ (open symbols) and $R_{s.dark}$ (closed symbols) on current density for 3 different UNSW one-sun Si solar cells. For each cell $R_{s.light}$ is shown for AM1.5 illumination. The BC cell was additionally measured at 0.5 and 1.5 suns.

3.3 Accuracy of the Method

As mentioned in Section 2, our method uses the J_{sc}-V_{oc} curve to approximate the unknown R_s-corrected *I-V* curve of the cell. The degree of accuracy of this approach strongly depends on the specific type of photovoltaic device under test. Therefore, a general assessment of the accuracy of our method is not possible. Instead, we will briefly discuss the uncertainties for the silicon solar cell measurements reported in Section 3.2.

According to Eqns. 5 and 6, the determination of $R_{s.light}$ and $R_{s.dark}$ requires the measurement of illuminated and dark *I-V* curves. Errors in the determination of these curves arise from the resolution of the voltmeter and ammeter, the stability of cell temperature, and from light intensity fluctuations. At UNSW, the main current uncertainty arises from light intensity fluctuations (≤ 0.1 mA/cm^2). Compared to this value, the resolution error of our ammeter (< 10 μA while measuring mA) is negligible. Due to the exponential diode characteristics, the impact of the lamp fluctuations on cell voltage is negligible. For accurate voltage measurements, the *I-V* curves are measured with the "4-point probe technique" (this eliminates the impact of probe contact resistances). The minimum voltage uncertainty is given by the resolution of the used voltmeter (0.2

mV). A more severe voltage error arises from an increased cell temperature in illuminated *I-V* measurements. At UNSW, under steady-state AM1.5 illumination, cell temperature is found to be increased by about 0.3°C for PERL-type cells, compared to dark *I-V* measurements. Above one sun, the temperature deviation increases approximately linearly with light intensity, while it is found to be negligible below 0.5 suns [14]. As the output voltage of Si solar cells reduces by ≈ 1.6 mV/K, the cell voltage in the one-sun measurements of Section 3.2 is reduced by about 0.5 mV. Thus, the total voltage uncertainty in our one-sun *I-V* curves is below 1 mV. Error analysis of Eqns. 5 and 6 for one-sun conditions (i.e., J ≈ 40 mA/cm^2) shows that the main R_s uncertainty arises from the voltage error and that a voltage uncertainty of 1 mV transfers to a R_s error of ± 0.03 Ωcm^2.

Additional uncertainty arises from approximating the unknown R_s-corrected *I-V* curve of the cell by the J_{sc}-V_{oc} curve. For the determination of $R_{s.dark}$, this approximation is valid to a high degree of accuracy (see Section 2.3), so that the total uncertainty of the $R_{s.dark}$ values reported in this work is about ± 0.03 Ωcm^2. For the determination of $R_{s.light}$, the J_{sc}-V_{oc} approximation is less ideal (see Section 2.3). If the saturation current J_0 does not strongly depend on the voltage across the cell (as is the case for the PESC cell and the buried-contact cell), the uncertainty in the determined value of $R_{s.light}$ near the maximum power point is estimated to be smaller than ± 0.05 Ωcm^2. Larger $R_{s.light}$ errors occur if J_0 depends strongly on the cell voltage (e.g. in PERL cells, see Section 2.3).

4. CONCLUSIONS

Although resistive losses in solar cells are distributed by nature, they can adequately be assessed in terms of a "*lumped series resistance model*" using the simple equivalent circuit of Fig. 2. The new measurement technique presented in this work uses the measured "J_{sc}-V_{oc} *curve*" of the device as an approximation to the unknown R_s-corrected *I-V* curve of the cell and determines the series resistance in dark and illuminated operating conditions ($R_{s.dark}$ and $R_{s.light}$) from the voltage shift between the J_{sc}-V_{oc} curve and the dark and illuminated *I-V* curve, respectively. As no assumptions on the properties of the diode (e.g., single or double-diode model, exponential *I-V* curve) in the equivalent circuit of Fig. 2 have to be made, our method is applicable to a large variety of photovoltaic devices.

In practical devices, owing to multi-dimensional effects, the lumped series resistance usually depends on the operating condition (i.e., dark or illuminated *I-V* measurements) and on the current density flowing through the device. Furthermore, for a given light intensity, $R_{s.light}$ of high-efficiency silicon solar cells is found to decrease when the cell operating voltage is increased from short-circuit towards open-circuit conditions. Experimentally, $R_{s.light}$ at the maximum power point is found to be significantly larger than $R_{s.dark}$. Thus, the assessment of resistive losses in a solar cell should generally be based on the determination of $R_{s.light}$ near the maximum power point, while the additional determination of $R_{s.dark}$ can provide valuable diagnostic information on the relative importance of the various sources of ohmic losses .

This work not only provides a new, powerful method for the determination of the lumped series resistance of photovoltaic devices, but also considerably improves the general understanding of ohmic power loss effects in Si solar cells.

Acknowledgments

The Centre for Photovoltaic Devices and Systems at the University of New South Wales is supported by the Australian Research Council's Special Research Centres Scheme and Pacific Power. The experimental devices reported in this work were made by X. Dai, A. Wang, Dr. J. Zhao and the Pilot Line Team within the Centre. One of the authors (A.G.A) gratefully acknowledges the support of a Feodor Lynen Fellowship provided by the German Alexander von Humboldt Foundation and fruitful discussions with Dr. A. Blakers, Australian National University, Canberra. Finally, we would like to thank Dr. G. Heiser from the School of Computer Science and Engineering at UNSW for his help with the 2D-simulations.

References

1 M. Wolf, "*Limitations and possibilities for improvement of photovoltaic solar energy converters*", Proc. IRE **48**, 1246, 1960.
2 J.J Wysocki, "*The effect of series resistance on photovoltaic solar energy conversion*", RCA Rev. **22**, 57, 1961.
3 R.J. Handy, "*Theoretical analysis of the series resistance of a solar cell*", Solid-State Electronics **10**, 765, 1967.
4 N.C. Wyeth, "*Sheet resistance components of series resistance in a solar cell as a function of grid geometry*", Solid-State Electr. **20**, 629, 1977.
5 J.L. Boone and T.P. Van Doren, "*Solar-cell design based on a distributed diode analysis*", IEEE Trans. Electr. Dev. **25**, 767, 1978.
6 L.D. Nielsen, "*Distributed series resistance effects in solar cells*", IEEE Trans. Electr. Dev. **29**, 821, 1982.
7 A. Cuevas, G.L. Araújo and J.M. Ruiz, "*Variation of the internal series resistance with the operating conditions of a solar cell: dark and illuminated cases*", Proc. 5th European Communities Photovoltaic Solar Energy Conference, Athens 1983, p.114.
8 A.G. Aberle, S.R. Wenham, M.A. Green and G. Heiser, "*Decreased emitter sheet resistivity loss in high-efficiency silicon solar cells*", Submitted to Progress in Photovoltaics, April 1993.
9 A. Rohatgi, J.R. Davis, R.H. Hopkins, P. Rai-Choudhury, P.G. McMullin and J.R. McCormick, "*Effect of titanium, copper and iron on silicon solar cells*", Solid-State Electronics **23**, 415, 1980.
10 M.A. Green, C.M. Chong, F. Zhang, A. Sproul, J. Zolper and S.R. Wenham, "*20% efficient laser grooved, buried contact silicon solar cells*", Proc. 20th IEEE Photovoltaic Specialists Conference, Las Vegas, 411, 1988.
11 S.R. Wenham, "*Buried-contact silicon solar cells*", Progress in Photovoltaics **1**, 3, 1993.
12 S.M. Sze, *Physics of Semiconductor Devices*, (Wiley, New York, 1982).
13 M.A. Green, *High Efficiency Silicon Solar Cells*, (Trans Tech Publications, Aedermannsdorf, Switzerland, 1987).
14 A.G. Aberle, S.J. Robinson, A. Wang, J. Zhao, S.R. Wenham and M.A. Green, "*High-efficiency silicon solar cells: fill factor limitations and non-ideal diode behaviour due to voltage-dependent rear surface recombination velocity*", Progress in Photovoltaics **1**, 133, 1993.
15 Simul Manual, Integrated Systems Lab, ETH Zurich, Switzerland, 1992.
16 M.A. Green, A.W. Blakers, S. Narayanan and M. Taouk, "*Improvements in silicon solar cell efficiency*", Solar Cells **17**, 75, 1986
17 A. Wang, J. Zhao and M.A. Green, "*24% efficient silicon solar cells*", Appl. Phys. Lett. **57**, 602, 1990.